

# The Electrochemical Properties of 1-Pyrenebutyric Acid/Graphene Composites and Their Application in Glucose Biosensors

Min Wang, Jiong Wang, Fengbin Wang, Xinghua Xia\*

(State Key Laboratory of Analytical Chemistry for Life Science, School of Chemistry and Chemical Engineering, Nanjing University, Nanjing 210093, China)

**Abstract:** The electrochemical properties of 1-pyrenebutyric acid/graphene composites (PBA/G) obtained by one-step synthesis via  $\pi$ - $\pi$  stacking was investigated. The electrochemical impedance titration curve shows the surface charge changes as function of solution pH by using ferricyanide/ferrocyanide redox couple as the probe. An apparent  $pK_a$  value is estimated as 6.2 according to the impedance titration curve. In addition, a glucose biosensor was constructed by immobilizing glucose oxidase (GOD) on the surface of PBA/G via covalent interaction. This biosensor shows a linear response to glucose within the concentration up to  $5 \text{ mmol} \cdot \text{L}^{-1}$  with a detection limit of  $0.085 \text{ mmol} \cdot \text{L}^{-1}$ . A small apparent Michaelis-Menten constant ( $5.40 \text{ mmol} \cdot \text{L}^{-1}$ ) of the immobilized GOD suggests that the immobilized GOD retains its bioactivity and shows high catalytic activity to glucose.

**Key words:** 1-pyrenebutyric acid; graphene; glucose oxidase; electrochemical biosensor; glucose

**CLC Number:** O646

**Document Code:** A

## 1 Introduction

Recently, two-dimensional graphene nanosheets have attracted extensive interest due to its extraordinary mechanical, thermal and electronic properties. They have the potential for a wide range of applications such as ultracapacitors<sup>[1]</sup>, chemical sensors and biosensors<sup>[2-3]</sup>, hydrogen storage<sup>[4]</sup> and field-effect transistors<sup>[5]</sup>. Graphene sheets have been synthesized by different methods such as chemical vapor deposition, epitaxial growth, reduction of graphene oxide sheets and carbon nanotube cutting<sup>[6-7]</sup>. Two key challenges in the synthesis of graphene sheets are the availability in large quantities and the prevention of irreversible aggregation. Nowadays, large-scale production of graphene sheets could be accomplished by the reduction of graphene oxide sheets. However, most resultant graphene sheets tend to form agglomerates or even restack to form graphite

via van der Waals interaction, which significantly limits the applications of graphene in many fields. In order to resolve this problem, graphene nanocomposites were prepared by combining graphene sheets with biocompatible molecules including surfactants, polymers, DNA and proteins<sup>[8-11]</sup>. This approach holds great promise for the bioassay applications because of their good water-solubility and versatile functional groups<sup>[12-15]</sup>.

1-pyrenebutyric acid (PBA), an organic fluorescent probe, provides potential applications in labeling macromolecules<sup>[16]</sup> and synthesizing biosensor materials<sup>[17]</sup> due to its outstanding optical and chemical stability. With the strong affinity to the basal plane of graphite via  $\pi$ - $\pi$  stacking, 1-pyrenebutyric acid has been immobilized on graphene sheets to obtain 1-pyrenebutyric acid/graphene composites (PBA/G)<sup>[18]</sup>. The resulting composites have good wa-

Received: 2012-06-26, Revised: 2012-08-17 \*Corresponding author, Tel: (86-25)83597436, E-mail: xhxia@nju.edu.cn

This work was financially supported by the National 973 Basic Research Program (No. 2012CB933804), the National Natural Science Foundation of China (No. 21035002, No. 21121091) and the Natural Science Foundation of Jiangsu province (No. BK2010009).

ter-solubility and could be widely used for graphene-based biosensors. Gao et al. constructed an enzyme-based signal-on DNA sensor for the specific detection of target DNA down to attomolar level with PBA/G as a nanoprobe substrate<sup>[19]</sup>. Liu et al. demonstrated a novel electrochemical biosensor for pathogenic virus detection based on the pyrene derivatives/graphene composites<sup>[20]</sup>. Obviously, it is important to understand the electrochemical properties of PBA/G and explore their applications further in the biosensors area.

In this work, the electrochemical properties of PBA/G were investigated by electrochemical techniques and a glucose biosensor based on PBA/G was constructed. PBA/G was synthesized and characterized by UV-vis spectroscopy and Raman spectroscopy. The surface charge of PBA/G in different pH values was investigated by electrochemical impedance titration. In addition, the performance of the glucose biosensor was characterized using amperometry and the apparent Michaelis-Menten constant of the immobilized GOD was obtained by the Lineweaver-Burk plots.

## 2 Experimental

### 2.1 Materials

Natural graphite powder (99.9995%, 100 mesh) was obtained from Alfa Aesar Company. 1-pyrenebutyric acid (PBA), glucose oxidase (GOD, from *Aspergillus niger*, 158 900 units · g<sup>-1</sup>), N-Ethyl-N-(3-dimethyl-aminopropyl) carbodiimide hydrochloride (EDC) and N-hydroxysuccinimide (NHS) were purchased from Sigma-Aldrich. All other reagents were of analytical grade.

### 2.2 Instruments

UV-vis absorption spectra were recorded on a UV 3600 spectrophotometer (Shimadzu, Japan). Raman scattering measurements were performed on a Renishaw InVia micro-Raman system (Renishaw, England) with an excitation wavelength of 514 nm. Electrochemical impedance spectroscopy (EIS) measurements were carried out with an Autolab PG-STAT 302 (Metrohm, Switzerland). Other electro-

chemical measurements were performed on a CHI 660D electrochemical working station (CH instruments, USA) using a three-electrode system with a modified glassy carbon (GC) electrode (3 mm in diameter) as the working electrode. A platinum wire and an Ag/AgCl reference electrode (saturated KCl) were used as the counter and reference electrodes, respectively.

### 2.3 Preparation of PBA/G Composites

Graphene oxide (GO) was synthesized from spectral graphite according to a modified Hummer's method<sup>[21]</sup>. PBA/G was fabricated by the reduction of GO in the presence of PBA according to the reported method<sup>[18]</sup>. In detail, 29 mg PBA was dissolved by 6 mL NaOH (83.3 mmol · L<sup>-1</sup>) solution and then 0.1 mg · mL<sup>-1</sup> GO suspension was added to the above solution. The resulting mixture was reduced with hydrazine solution at 80 °C under vigorous agitation for 24 h. The product PBA/G was centrifuged, thoroughly washed with dilute NaOH solution and ultra-pure water respectively and then dried under vacuum at room temperature. As a comparison, graphene was fabricated by the same procedure without addition of PBA.

### 2.4 Preparation of GOD/PBA/G Modified GC Electrodes

Glassy carbon (GC) electrode was well polished with 0.05 μm alumina slurry, and then cleaned ultrasonically in ethanol and water for 3 min, respectively. The PBA/G and graphene modified GC electrodes were prepared by casting 10 μL PBA/G or graphene suspension onto the pretreated bare GC electrode using a micropipette tip and dried in air. The PBA/G modified GC electrode was immersed in 0.1 mol · L<sup>-1</sup> phosphate buffer (pH 7.4) containing 0.15 mol · L<sup>-1</sup> EDC and 0.3 mol · L<sup>-1</sup> NHS for 1 h to activate the —COOH groups in PBA/G. GOD was covalently attached to PBA/G by incubating the activated PBA/G modified GC electrode in 10 mg · mL<sup>-1</sup> GOD solution for 1 h.

### 3 Results and Discussion

#### 3.1 Characterization of the Graphene and PBA/G

Fig. 1A shows the UV-vis absorption spectra of PBA, PBA/G and the centrifugal supernatants. Consistent with literature<sup>[22]</sup>, the main absorption peaks of PBA appear at 242 nm, 276 nm and 342 nm. Here PBA was decorated on graphene sheets via  $\pi$ - $\pi$  stacking and the unbound PBA was removed by several cycles of centrifugation and wash with dilute NaOH solution. The observed absorbance peaks of PBA in the spectra of the centrifugal supernatants are weakened gradually and disappear after the third wash, which demonstrates that the unbound PBA was removed thoroughly. As depicted in the inset of Fig. 1A, these characteristic peaks of PBA observed in the spectrum of PBA/G are red-shifted (250 nm, 286 nm and 354 nm), which is attributed to the  $\pi$ - $\pi$  stacking interaction between PBA and graphene. The Raman spectra of PBA and PBA/G are shown in Fig. 1B. Compared to the spectra of GO and graphene, the shoulder band around 1610  $\text{cm}^{-1}$  and the weak band at 1235  $\text{cm}^{-1}$  in the spectrum of PBA/G indicate the formation of PBA/G nanocomposites. As shown in Tab. 1, the D/G ratio of PBA/G increases in comparison with that of GO, which is consistent with that report previously<sup>[18]</sup>.

#### 3.2 Electrochemical Properties of PBA/G

The surface properties of graphene and PBA/G modified GC electrodes were characterized in  $\text{K}_3\text{Fe}(\text{CN})_6$  solution by cyclic voltammograms (CVs). As shown in Fig. 2 (curve a), the graphene modified GC electrode shows a couple of well-defined redox

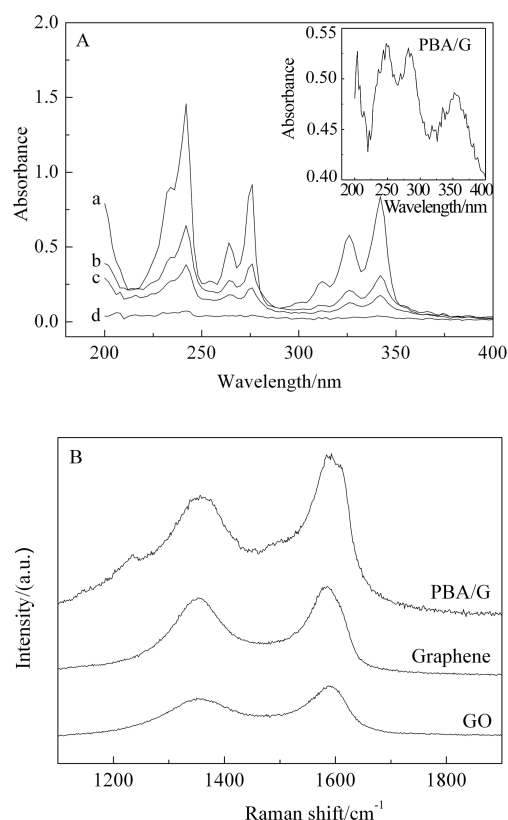


Fig. 1 A. UV-vis absorption spectra of PBA (a), PBA/G (inset) and the centrifugal supernatants (b. 1st wash; c. 2nd wash; d. 3rd wash). B. Raman spectra of GO, graphene and PBA/G.

wave ( $\Delta E_p = 108$  mV,  $i_{pd}/i_{pa} \approx 1$ ) due to the excellent conductivity of graphene. However, no obvious reversible redox wave is observed for the PBA/G modified GC electrode (Fig. 2, curve b), which is attributed to the electrostatic repulsion between the carboxylate groups of PBA/G and the  $\text{Fe}(\text{CN})_6^{3-}$  probe<sup>[20]</sup>. This result demonstrates that the surface of PBA/G is negatively charged under these conditions.

Electrochemical impedance titration is useful

Tab. 1 Raman bands of GO, graphene and PBA/G

Sample	D-band/ $\text{cm}^{-1}$	G-band/ $\text{cm}^{-1}$	D/G ratio	A shoulder band/ $\text{cm}^{-1}$	Another weak band/ $\text{cm}^{-1}$
GO	1355	1591	0.72	—	—
Graphene	1354	1585	0.87	—	—
PBA/G	1358	1588	0.74	ca. 1610	1235

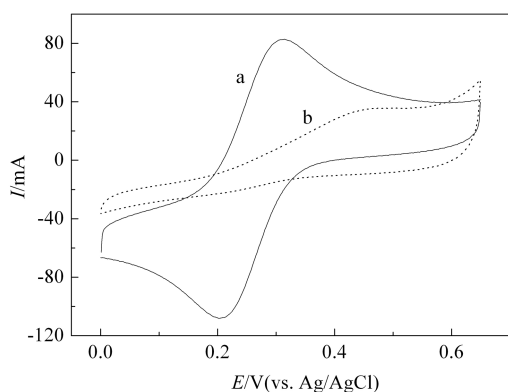


Fig. 2 CVs of graphene (a) and PBA/G (b) modified GC electrodes in  $10 \text{ mmol} \cdot \text{L}^{-1} \text{K}_3\text{Fe}(\text{CN})_6$  solution containing  $0.5 \text{ mol} \cdot \text{L}^{-1} \text{KCl}$ . The scan rate was  $50 \text{ mV} \cdot \text{s}^{-1}$ .

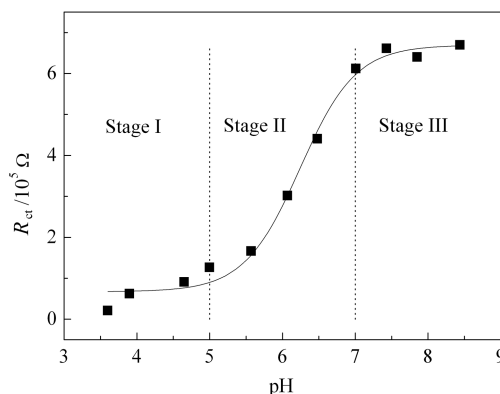


Fig. 3 Electrochemical impedance titration curve of the PBA/G modified GC electrode in  $1.0 \text{ mmol} \cdot \text{L}^{-1} \text{K}_3[\text{Fe}(\text{CN})_6]$  and  $1.0 \text{ mmol} \cdot \text{L}^{-1} \text{K}_4[\text{Fe}(\text{CN})_6]$  (1:1) solution containing  $10 \text{ mmol} \cdot \text{L}^{-1}$  phosphate buffer (different pH values) and  $0.1 \text{ mol} \cdot \text{L}^{-1} \text{KCl}$ . Electrochemical impedance spectra were carried out under open-circuit conditions. The AC voltage amplitude was  $5 \text{ mV}$  and the frequencies ranged from  $0.01 \text{ Hz}$  to  $10^5 \text{ Hz}$ .

to investigate the surface charges of PBA/G and meanwhile obtain the apparent  $\text{pK}_a$  from the titration curve.  $[\text{Fe}(\text{CN})_6]^{3-/4-}$  is used as the redox probe to investigate the surface charge of PBA/G. The carboxyl groups of PBA/G exhibit distinct state in different pH values, resulting in different charge-transfer resistance ( $R_{ct}$ ) values. At lower pH ( $<5$ ), the carboxyl groups of PBA/G are fully protonated, which hardly affects or inhibits the electron transfer between the probe and the electrode. As a result, the  $R_{ct}$  values changes slightly to show a short plateau (stage I in Fig. 3). With the increase of pH ( $5 \sim 7$ ), the carboxyl groups gradually deprotonate to yield a negatively charged carboxylate ion on the surface of modified electrode, which gradually increases the electrostatic repulsion between the probe and the negatively charged carboxylate groups and inhibits interfacial electron transfer. Therefore, the  $R_{ct}$  values increase with solution pH (stage II in Fig.3). At higher solution pH ( $>7$ ), the carboxyl groups are fully deprotonated and the electrostatic repulsion between the probe and the electrode reaches maximum. Thus another plateau is observed (stage III in Fig. 3). The resultant electrochemical impedance titration curve represents the change in surface charge with solution pH. According to the responding pH value of the midpoint of the titration curve<sup>[23]</sup>, an apparent  $\text{pK}_a$  value of PBA/G could be estimated to be 6.2 which is larger than that of PBA in the so-

lution (ca.  $4.8^{[24]}$ ). This may be due to the coexistence of the graphene sheets which delocalizes the charges from PBA.

### 3.3 Glucose Biosensors Based on PBA/G Composites

Glucose oxidase (GOD) could catalyze the oxidation of glucose to produce  $\text{H}_2\text{O}_2$  in the presence of  $\text{O}_2$  and has been widely used in construction of glucose biosensors<sup>[25-26]</sup>. In the present work, GOD, as a model enzyme, was immobilized on the surface of PBA/G by covalent modification to construct a glucose biosensor. Fig. 4 shows the impedance spectra (Nyquist plots) corresponding to the stepwise modification processes. The  $R_{ct}$  ( $42.22 \text{ k}\Omega$ , Fig. 4b) of the PBA/G modified GC electrode was much larger than that of the bare GCE ( $151.4 \Omega$ , Fig. 4a), suggesting that the successfully formation of PBA/G membrane which can hinder the electron transfer from the redox probe of  $[\text{Fe}(\text{CN})_6]^{3-/4-}$ . When GOD was immobilized via covalent interaction, the  $R_{ct}$  of the resultant GOD/PBA/G film ( $67.62 \text{ k}\Omega$ , Fig. 4c) increases largely, indicating that a glucose biosensor based on the PBA/G composites was successfully constructed.

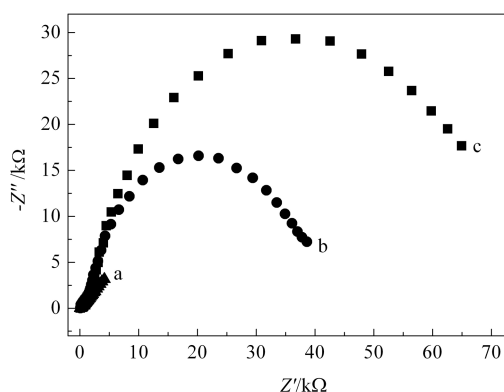


Fig. 4 Nyquist plots of the different electrodes in 2.5 mmol·L<sup>-1</sup> K<sub>3</sub>[Fe(CN)<sub>6</sub>] and 2.5 mmol·L<sup>-1</sup> K<sub>4</sub>[Fe(CN)<sub>6</sub>] (1:1) solution containing 0.1 mol·L<sup>-1</sup> KCl. a. Bare GC electrode; b. PBA/G modified GC electrode; c. GOD/PBA/G modified GC electrode.

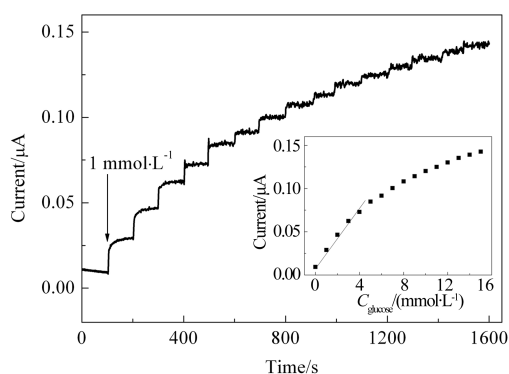


Fig. 5 Typical current time response curves of GOD/PBA/G modified GC electrode at 0.4 V in 0.1 mol·L<sup>-1</sup> phosphate buffer (pH 7.4) upon successive addition of 1 mmol·L<sup>-1</sup> glucose. Inset: relationship between response current and glucose concentration.

The performance of the resulting biosensor was tested by recording the amperometric response of the oxidation of hydrogen peroxide produced from the enzyme reaction (the detection potential: 0.4 V). As shown in Fig. 5, the positive current at the GOD/PBA/G modified GC electrode increases with the injected glucose (each addition of 1 mmol·L<sup>-1</sup>). The calibrated steady-current responses with glucose concentration are given in the inset of Fig. 5. The relationship is approximately linear up to 5 mmol·L<sup>-1</sup> with a detection limit of 0.085 mmol·L<sup>-1</sup>. The high affinity of GOD was found by the determination of the apparent Michaelis-Menten constant ( $K_m^{app}$ ) which can be estimated in terms of the Lineweaver-Burk equation<sup>[26]</sup>.

$$\frac{1}{i_{ss}} = \frac{1}{i_{max}} + \frac{K_m^{app}}{C i_{max}}$$

where,  $i_{ss}$  and  $i_{max}$  are the steady-state current and the maximum current, respectively.  $C$  is the glucose concentration. Fig. 6 shows the Lineweaver-Burk plots based on the data from the inset of Fig. 5. The  $i_{max}$  and determined from the slope and the intercept of the straight line in Fig. 6 are 0.18 μA and 5.40 mmol·L<sup>-1</sup>, respectively. The value is smaller than that of GOD immobilized by the other reported methods, which demonstrates that the immobilized GOD using our method possesses high catalytic activity with respect to glucose. In addition, the stability

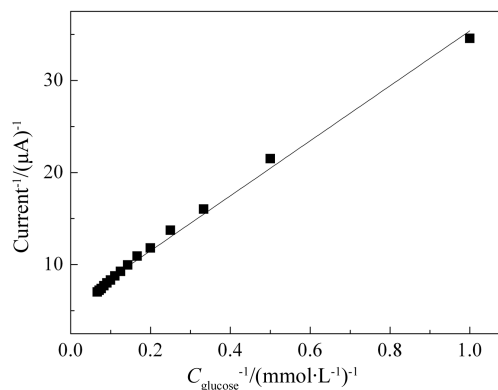


Fig. 6 Lineweaver-Burk plots based on the data in the inset of Fig. 5.

of the immobilized GOD was investigated in 0.1 mol·L<sup>-1</sup> phosphate buffer (pH 7.4) containing 1 mmol·L<sup>-1</sup> glucose with a detection potential of 0.4 V. The result shows the activity of the enzyme retains approximately 71% of its original value after a storage time of 16 h.

### 4 Conclusions

In summary, the electrochemical properties of water-soluble PBA/G composites were investigated by electrochemical techniques. The surface charge of PBA/G varied with the pH values of bulk solution and the apparent pK<sub>a</sub> of PBA/G determined from the electrochemical impedance titration curve is 6.2. A glucose biosensor based on PBA/G was constructed by attaching GOD on the surface of PBA/G via covalent interaction. This biosensor shows a linear re-

sponse to glucose in the concentration up to  $5 \text{ mmol} \cdot \text{L}^{-1}$  with a detection limit of  $0.085 \text{ mmol} \cdot \text{L}^{-1}$  and the small value ( $5.40 \text{ mmol} \cdot \text{L}^{-1}$ ) demonstrates that this biosensor shows high catalytic activity with respect to glucose. These results may inspire others for more applications of PBA/G composites in bioelectronics and biosensors.

## References:

- [1] Stoller M D, Park S, Zhu Y W, et al. Graphene-based ultracapacitors[J]. *Nano Letters*, 2008, 8(10): 3498-3502.
- [2] Schedin F, Geim A K, Morozov S V, et al. Detection of individual gas molecules adsorbed on graphene[J]. *Nature Materials*, 2007, 6(9): 652-655.
- [3] Zhou M, Zhai Y M, Dong S J. Electrochemical sensing and biosensing platform based on chemically reduced graphene oxide[J]. *Analytical Chemistry*, 2009, 81(14): 5603-5613.
- [4] Lee H, Ihm J, Cohen M L, et al. Calcium-decorated graphene-based nanostructures for hydrogen storage [J]. *Nano Letters*, 2010, 10(3): 793-798.
- [5] Gilje S, Han S, Wang M S, et al. A chemical route to graphene for device applications[J]. *Nano Letters*, 2007, 7(11): 3394-3398.
- [6] Park S, Ruoff R S. Chemical methods for the production of graphenes[J]. *Nature Nanotechnology*, 2009, 4(4): 217-224.
- [7] Shinde D B, Debgupta J, Kushwaha A, et al. Electrochemical unzipping of multi-walled carbon nanotubes for facile synthesis of high-quality graphene nanoribbons[J]. *Journal of the American Chemical Society*, 2011, 133(12): 4168-4171.
- [8] Zeng Q, Cheng J S, Tang L H, et al. Self-assembled graphene-enzyme hierarchical nanostructures for electrochemical biosensing[J]. *Advanced Functional Materials*, 2010, 20(19): 3366-3372.
- [9] Zhang Q, Qiao Y, Hao F, et al. Fabrication of a biocompatible and conductive platform based on a single-stranded DNA/graphene nanocomposite for direct electrochemistry and electrocatalysis[J]. *Chemistry-A European Journal*, 2010, 16(27): 8133-8139.
- [10] Kang X H, Wang J, Wu H, et al. Glucose oxidase-graphene-chitosan modified electrode for direct electrochemistry and glucose sensing[J]. *Biosensors and Bioelectronics*, 2009, 25(4): 901-905.
- [11] Wang M, Xiao F N, Wang K, et al. Electric field driven protonation/deprotonation of 3,4,9,10-perylene tetracarboxylic acid immobilized on graphene sheets via  $\pi-\pi$  stacking[J]. *Journal of Electroanalytical Chemistry*, 2012, in press: doi: <http://dx.doi.org/10.1016/j.jelechem.2012.07.036>.
- [12] Wang Y, Shao Y Y, Matson D W, et al. Nitrogen-doped graphene and its application in electrochemical biosensing[J]. *ACS Nano*, 2010, 4(4): 1790-1798.
- [13] Chen D, Tang L, Li J H. Graphene-based materials in electrochemistry[J]. *Chemical Society Review*, 2010, 39(8): 3157-3180.
- [14] Wang Y, Li Z H, Wang J, et al. Graphene and graphene oxide: Biofunctionalization and applications in biotechnology[J]. *Trends in Biotechnology*, 2011, 29(5): 205-212.
- [15] Zhang Q, Wu S, Zhang L, et al. Fabrication of polymeric ionic liquid/graphene nanocomposite for glucose oxidase immobilization and direct electrochemistry[J]. *Biosensors and Bioelectronics*, 2011, 26(5): 2632-2637.
- [16] Chen S H, Duhamel J, Bahun G J, et al. Quantifying the presence of unwanted fluorescent species in the study of pyrene-labeled macromolecules[J]. *Journal of Physical Chemistry B*, 2011, 115(33): 9921-9929.
- [17] Chen R J, Zhang Y G, Wang D W, et al. Noncovalent sidewall functionalization of single-walled carbon nanotubes for protein immobilization[J]. *Journal of the American Chemical Society*, 2001, 123(16): 3838-3839.
- [18] Xu Y X, Bai H, Lu G W, et al. Flexible graphene films via the filtration of water-soluble noncovalent functionalized graphene sheets[J]. *Journal of the American Chemical Society*, 2008, 130(18): 5856-5857.
- [19] Gao W C, Dong H F, Lei J P, et al. Signal amplification of streptavidin-horseradish peroxidase functionalized carbon nanotubes for amperometric detection of attomolar DNA[J]. *Chemical Communications*, 2011, 47: 5220-5222.
- [20] Liu F, Choi K S, Park T J, et al. Graphene-based electrochemical biosensor for pathogenic virus detection[J]. *BioChip Journal*, 2011, 5(2): 123-128.
- [21] Guo H L, Wang X F, Qian Q Y, et al. A green approach to the synthesis of graphene nanosheets[J]. *ACS Nano*, 2009, 3(9): 2653-2659.
- [22] Guldi D M, Rahman G M A, Jux N, et al. Functional single-wall carbon nanotube nanohybrids associating SWNTs with water-soluble enzyme model systems[J]. *Journal of the American Chemical Society*, 2005, 127(27): 9830-9838.
- [23] Zhao J W, Luo L Q, Yang X R, et al. Determination of surface  $\text{pK}_a$  of SAM using an electrochemical titration method[J]. *Electroanalysis*, 1999, 11(15): 1108-1113.

- [24] Tulock J J, Blanchard G J. Role of probe molecule structure in sensing solution phase interactions in ternary systems[J]. *The Journal of Physical Chemistry A*, 2000, 104 (36): 8340-8345.
- [25] Hu L Z, Han S, Liu Z Y, et al. A versatile strategy for electrochemical detection of hydrogen peroxide as well as related enzymes and substrates based on selective hydrogen peroxide-mediated boronate deprotection [J]. *Electrochemistry Communications*, 2011, 13(12): 1536-1538.
- [26] Jia W Z, Wang K, Zhu Z J. et al. One-step immobilization of glucose oxidase in a silica matrix on a Pt electrode by an electrochemically induced sol-gel process[J]. *Langmuir*, 2007, 23(23): 11896-11900.

## 1-苾丁酸/石墨烯复合物的电化学性质及其在葡萄糖传感器上的应用

王 敏, 王 炯, 王凤彬, 夏兴华\*

(南京大学 化学化工学院, 生命分析化学国家重点实验室, 江苏 南京 210093)

**摘要:** 本文采用一步法制备了 1-苾丁酸/石墨烯复合物(PBA/G), 并研究了它的电化学性质. 采用铁氰化钾和亚铁氰化钾电化学探针测定了其电化学阻抗滴定曲线, 确定了 PBA/G 的表观  $pK_a$  为 6.2. 此外, 将葡萄糖氧化酶(GOD)共价键合在 PBA/G 表面构建了葡萄糖电化学传感器, 其电化学响应与葡萄糖浓度( $5 \text{ mmol} \cdot \text{L}^{-1}$  浓度范围内)呈线性关系, 检测限为  $0.085 \text{ mmol} \cdot \text{L}^{-1}$ . 实验还测定了固定在 PBA/G 表面的 GOD 的表观米氏常数为  $5.40 \text{ mmol} \cdot \text{L}^{-1}$ , 表明固定化的 GOD 对葡萄糖有较高的催化活性.

**关键词:** 1-苾丁酸; 石墨烯; 葡萄糖氧化酶; 电化学生物传感器; 葡萄糖